

Pushbroom Microwave Radiometer Results from HAPEX-MOBILHY

William E. Nichols,^{*} Richard H. Cuenca,[†] Thomas J. Schmugge,[‡] and James R. Wang[§]

The NASA C-130 remote sensing aircraft was in Toulouse, France from 25 May through 4 July 1986, for participation in the HAPEX-MOBILHY program. Spectral and radiometric data were collected by C-130-borne sensors in the visible, infrared, and microwave wavelengths. These data provided information on the spatial and temporal variations of surface parameters such as vegetation indices, surface temperature, and surface soil moisture. The Pushbroom Microwave Radiometer (PBMR) was used to collect passive microwave brightness temperature data. This four-beam sensor operates at the 21-cm wavelength, providing cross-track coverage approximately 1.2 times the aircraft altitude. Observed brightness temperatures for the period were high, ranging from above 240 K to about 290 K. Brightness temperature images appeared to correspond well to spatial and temporal soil moisture variation. Previous research has demonstrated that an approximately linear relationship exists between the surface emissivity and surface soil moisture. For these data, however, regression analysis did not indicate a strong linear relationship ($r^2 = 0.32$ and $r^2 = 0.42$, respectively) because of the limited range of soil moisture conditions encountered and the small number of ground measurements. When results from wetter soil conditions encountered in another experiment were included, the regression improved dramatically. Based on similar research with the PBMR and an understanding of the ground data

collection program, this result was examined to produce recommendations for improvements to future passive microwave research and data collection programs. Examples of surface soil moisture maps generated with PBMR data are presented which appear to be representative of the actual soil moisture conditions.

INTRODUCTION

The HAPEX-MOBILHY Program

The HAPEX-MOBILHY (Hydrologic Atmospheric Pilot Experiment—Modélisation du Bilan Hydrique) program was directed at study of the hydrologic budget and evaporation flux at the scale of a General Circulation Model grid cell, that is, 10^4 km² (André et al., 1986; 1988). Different surface and subsurface measurement networks were operated from mid-1985 through early 1987 to measure and monitor solid moisture, surface energy flux, surface hydrology, and atmospheric properties. A Special Observing Period (SOP) was conducted from 7 May through 15 July 1986. Detailed measurements of atmospheric fluxes and remotely sensed measurements of surface properties were collected during the SOP using three instrumented aircraft, one of which was the NASA C-130 remote sensing aircraft. The Pushbroom Microwave Radiometer (PBMR) was among the instruments aboard the NASA C-130 during the SOP. This sensor operates at a 21-cm wavelength (frequency = 1.413 GHz) and was used to measure surface brightness temperatures at selected sites in the HAPEX-MOBILHY grid.

The subject of this article is the temporal and spatial mapping of soil moisture observed with the PBMR during the HAPEX-MOBILHY SOP. Closely associated with this task is examination of the correlation between remote passive microwave measurements and direct measurements of surface soil moisture.

^{*}Geosciences Department, Pacific Northwest Laboratory, Richland, Washington

[†]Department of Bioresource Engineering, Oregon State University, Corvallis

[‡]USDA Agricultural Research Service, Beltsville, Maryland

[§]NASA Goddard Space Flight Center, Greenbelt, Maryland

Address correspondence to W. E. Nichols, Battelle Pacific Northwest Laboratories, P.O. Box 999 MSIN K6-77, Richland, WA 99352.

Received 31 July 1992; revised 16 January 1993.

Passive Microwave Measurement of Soil Moisture

A passive microwave radiometer measures the thermal microwave emission from a surface. At microwave wavelengths, the intensity of the surface emission is proportional to the product of the kinetic, or physical temperature (T_{soil}) and the emissivity (e) of the surface (the Rayleigh-Jeans approximation). This product is commonly called the brightness temperature (T_B) of a surface, expressed in Kelvins:

$$T_B = e T_{\text{soil}}. \quad (1)$$

To compute emissivity, the brightness temperature measured with a radiometer is divided by the kinetic temperature of the surface measured or estimated by some other means.

The use of emissivity for estimation of surface soil moisture is based on the sensitivity of a soil's dielectric properties to its moisture content. For the frequency at which the PBMR operates, the dielectric constant is about 3.5 for a dry soil and 80 for water. The addition of water to soil increases the soil's dielectric constant considerably, resulting in an emissivity shift from 0.95 for dry soils to less than 0.70 for wet soils. Emissivity is influenced by such surface factors as roughness and vegetation cover (Theis and Blanchard, 1988). A range of vegetation conditions was encountered in the HAPEX-MOBILHY experiment, ranging from a microwave-opaque pine forest to bare soils. Jackson and O'Neill (1987) found that salinity, though theoretically held to have an effect on the microwave emissions of soils, did not appear to be important for general applications in interpreting soil moisture under most agricultural conditions. The thickness of a soil layer for which the emissivity is measured by a passive microwave radiometer is roughly a few tenths of a wavelength (Jackson and Schmugge, 1986). For the 21-cm wavelength PBMR sensor, this is about 2–5 cm.

The Pushbroom Microwave Radiometer

The PBMR is a four-beam radiometer operating at a center frequency of 1.413 GHz (21-cm wavelength, or L-band) with beams centered to $\pm 8^\circ$ and $\pm 24^\circ$ from the nadir. The relative sensitivity of the sensor is 1 K and the absolute accuracy is approximately 2 K. The antenna receives horizontally polarized radiation. The total cross-track coverage is about 1.2 times the aircraft altitude. Figure 1 depicts the ground coverage of the PBMR sensor and the relative position of the beam centers. Note that the flight direction is into the plane of the paper for Figure 1, so that beam 1 is to the right of the flight line. PBMR measurements and the time of measurement from an onboard clock are recorded onto magnetic media.

The PBMR has been used extensively in passive microwave research since it was developed at the NASA

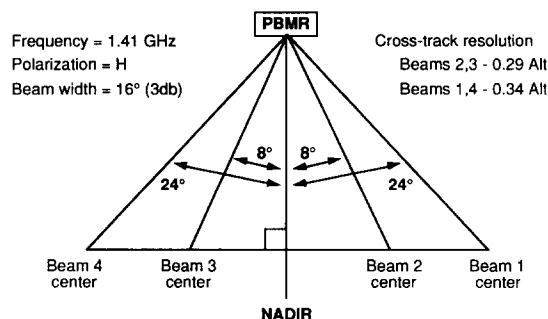


Figure 1. Sensor geometry of the Pushbroom Microwave Radiometer.

Langley Research Center. Jackson et al. (1986) demonstrated use of the sensor in mapping pre-planting soil moisture in Texas. The PBMR has been used in both the HAPEX-MOBILHY and the FIFE large-scale field experiments (André et al., 1986; 1988; Schmugge et al., 1988; Wang et al., 1989; 1990).

MEASUREMENTS

Sensors aboard the NASA C-130 aircraft during its participation in the HAPEX-MOBILHY SOP included the Pushbroom Microwave Radiometer, the PRT-5 thermal infrared radiometer, the NS001 Thematic Mapper Simulator (TMS), the Thermal Infrared Multispectral Scanner (TIMS), and a nadir-viewing video camera which was used to ground-register PBMR data. The PRT-5 is a nadir-centered thermal infrared sensor used for surface temperature measurement. Its field of view is 0.04 times the aircraft altitude.

A map of the HAPEX-MOBILHY grid is shown in Figure 2. The C-130 flight paths are indicated, as well as the locations of the 12 sites at which the local surface energy balance was measured during the SOP at 15-min intervals using the SAMER (Station Automatique de Mesure de l'Evapotranspiration Réelle) system (Bessmoulin et al., 1987). Neutron probe soundings were collected at 7-day intervals at these 12 locations and two others to monitor profile soil moisture content (Goutorbe et al., 1989). Low-altitude PBMR coverage was obtained over the Lubbon (SAMER 1 and 5) and Castelnau (SAMER 10) sites in the HAPEX-MOBILHY grid. The nominal C-130 flight altitude for these missions was 300 m and 1500 m above ground level (agl).

Central Site Lubbon, located at latitude $44^\circ 07'N$, longitude $0^\circ 03'W$, and altitude 146 m above mean sea level (msl), is shown in detail in a digitized map (Fig. 3). The area depicted in Figure 3 is located around SAMER stations 1 and 5 in Figure 2, where four east-west 300 m C-130 flight lines are indicated in Figure 2. This site received the most intensive coverage of any

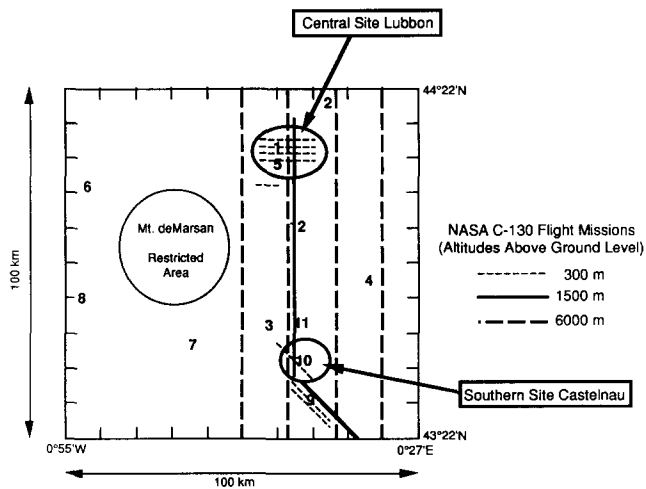


Figure 2. Map of the HAPEX-MOBILHY program grid, located in southwest France roughly between Toulouse and Bordeaux. SAMER station locations are indicated by their identification number (1–12) and NASA C-130 flight lines are shown by line types that indicate the nominal above-ground flight altitude.

HAPEX-MOBILHY site. Two SAMER stations were located at the positions shown in Figure 3 during the SOP. SAMER 01 (Lubbon 1) was in an oat field, and SAMER 05 (Lubbon 2) was in a maize field south of SAMER 01. Gravimetric soil moisture samples of the first 5 cm of soil were taken within ± 1 h of each C-130 overflight from six fields located in the area depicted by Figure 3. These fields are identified in Figure 3 as N0, N1, . . . , N5. Field N1 was a forest clearing, while the other five fields were planted with field crops (oats

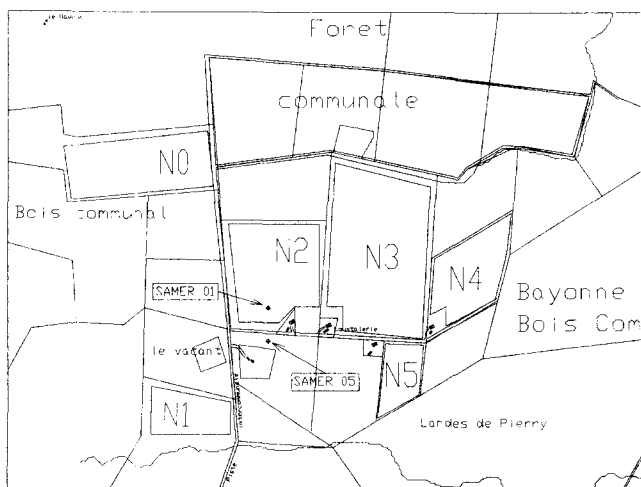


Figure 3. Map of Central Site Lubbon and vicinity. MAP depicts an area 4000 m \times 3000 m, which corresponds exactly to the brightness temperature imaging areas shown in Figures 4, 5, and 6, as well as the soil moisture maps shown in Figures 11, 12, and 13. Calibration fields are denoted by N0, N1, . . . , N5.

Table 1. Ground-Observed Surface Soil Moisture Values (Percent by Weight) for Central Site Lubbon Calibration Fields^a

| DOY | Statistic | N0 | N1 | N2 | N3 | N4 | N5 |
|--------|-----------|------|-------|------|------|------|------|
| 86D151 | \bar{x} | — | — | — | 9.0 | 9.8 | 9.5 |
| | s | — | — | — | 1.83 | 2.99 | 1.91 |
| 86D154 | \bar{x} | — | 15.8 | — | 7.0 | 12.0 | 9.3 |
| | s | — | 11.62 | — | 2.83 | 1.41 | 1.50 |
| 86D157 | \bar{x} | — | 10.3 | 8.3 | — | — | 9.3 |
| | s | — | 2.63 | 2.06 | — | — | 1.26 |
| 86D165 | \bar{x} | 10.0 | 6.5 | 4.8 | — | 3.0 | 4.5 |
| | s | 2.45 | 3.11 | 1.50 | — | 1.83 | 1.00 |
| 86D167 | \bar{x} | 5.3 | 7.8 | 3.8 | — | 6.5 | 4.5 |
| | s | 2.50 | 3.30 | 2.22 | — | 3.32 | 1.00 |
| 86D169 | \bar{x} | 5.5 | 5.8 | 2.0 | — | 4.3 | 2.0 |
| | s | 2.65 | 0.96 | 1.15 | — | 3.20 | 1.15 |
| 86D171 | \bar{x} | 3.0 | 5.3 | 3.5 | — | 2.8 | 0.9 |
| | s | 2.16 | 3.30 | 2.38 | — | 2.06 | 0.25 |
| 86D176 | \bar{x} | 3.8 | 5.8 | 1.8 | — | 1.3 | 1.4 |
| | s | 2.87 | 4.86 | 1.39 | — | 0.50 | 1.74 |
| 86D178 | \bar{x} | 3.0 | 13.0 | 1.9 | — | — | — |
| | s | 2.83 | 13.59 | 1.08 | — | — | — |
| 86D181 | \bar{x} | 7.5 | 8.5 | 2.5 | — | 8.8 | 8.8 |
| | s | 3.11 | 6.40 | 0.58 | — | 3.59 | 1.71 |
| 86D183 | \bar{x} | 2.8 | 5.5 | 1.8 | — | 4.5 | 10.0 |
| | s | 0.50 | 2.65 | 1.50 | — | 2.89 | 4.76 |

^a $n = 4$ observations for all fields and dates monitored, \bar{x} = sample mean, and s = sample standard deviation.

Table 2. Summary Statistics for Surface Bulk Density (g/cm^3) Sample Measurements for Central Site Lubbon Calibration Fields^a

| Statistic | Calibration Field | | | | | |
|-----------|-------------------|-------|-------|-------|-------|-------|
| | N0 | N1 | N2 | N3 | N4 | N5 |
| \bar{x} | 1.237 | 1.488 | 1.217 | 1.370 | 1.263 | 1.306 |
| s | 0.040 | 0.165 | 0.046 | 0.119 | 0.023 | 0.070 |

^a \bar{x} = sample mean and s = sample standard deviation.

or maize). Table 1 lists summary statistics for the volumetric surface soil moisture samples. Soil bulk density was also sampled for these fields to permit conversion of gravimetrically determined water contents to volumetric basis; the summary statistics for these samples are listed in Table 2.

RESULTS

Brightness Temperature Image Processing

Using computer programs developed for this study (Nichols, 1989), PBMR data from the vicinity of Central Site Lubbon and Southern Site Castelnau were pro-

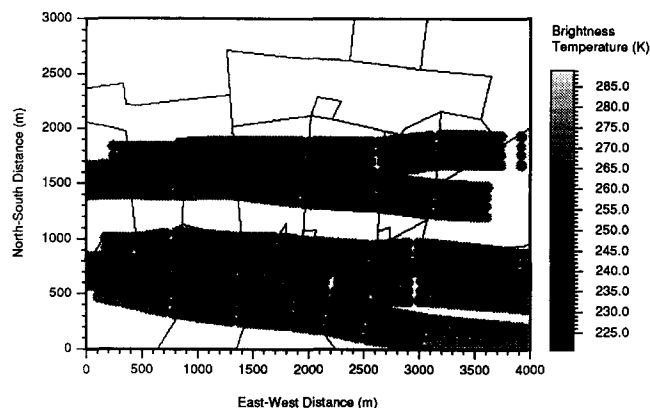


Figure 4. Brightness temperature image of Central Site Lubbon on 29 May 1986.

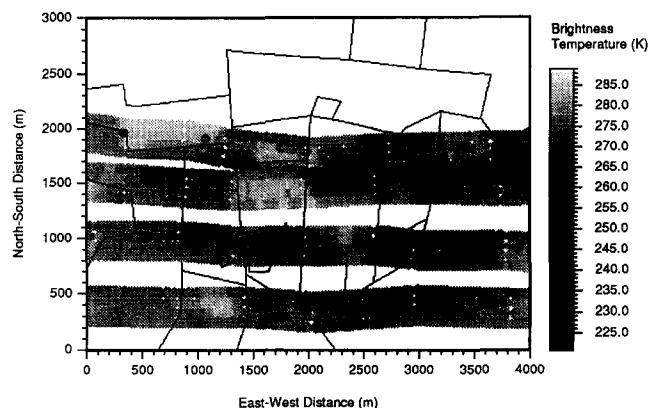
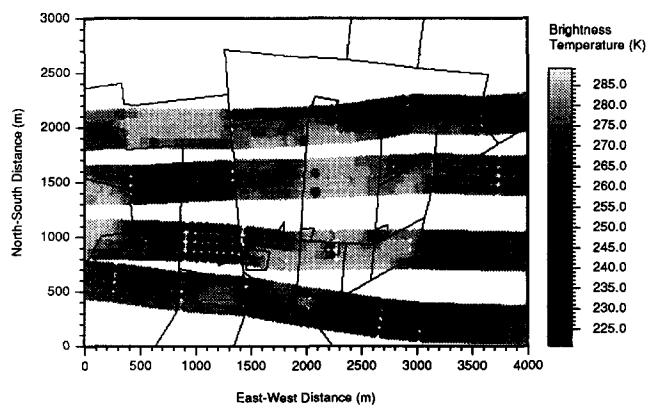


Figure 6. Brightness temperature image of Central Site Lubbon on 2 July 1986.

cessed to obtain brightness temperature imagery. Images were restricted to the same ground dimensions for each date to maintain consistency; 4000 m \times 3000 m for Lubbon and 2000 m \times 2000 m for Castelnau. The map in Figure 3 depicts the precise area of all Lubbon images, that is, the boundaries of the map correspond to the boundaries of all images presented in this article. This imaging area was selected to include all the ground-measured fields at Lubbon and most of the area viewed by the PBMR on the 300-m-altitude (agl) flight missions.

Three brightness-temperature images of Central Site Lubbon are shown for 29 May (Fig. 4), 16 June (Fig. 5), and 2 July (Fig. 6). These three were chosen from the larger collection of brightness temperature images to illustrate the variation apparent during the SOP. In viewing the images, recall that brightness temperature is negatively related to soil moisture, that is, lower brightness temperature implies higher soil moisture content. Brightness temperature values in Figures 4, 5, and 6 range from 225 K to 285 K, and are coded so that warmer (drier) areas appear dark, and cooler (wetter) areas appear light. The black lines represent

Figure 5. Brightness temperature image of Central Site Lubbon on 16 June 1986.



field boundaries digitized from Institut Géographique National (IGN) maps (compare to Fig. 3). Sensor coverage was typically 50% of the imaging area for Lubbon and 25% for Castelnau for the 300-m flights. Variations in flight lines caused slightly different portions of the image area to be mapped on different dates.

The brightness temperature images of Central Site Lubbon show a strong response to both spatial and temporal soil moisture variation. The temporal variation is apparent when comparing Figures 4, 5, and 6; there is a pronounced shift towards a drier surface soil moisture condition in the agricultural fields with each successive date. For example, in the first image (Fig. 4, 29 May) the cultivated areas in the central part of image have relatively low brightness temperatures ranging from 235 K to 265 K. These brightness temperatures were collected at the beginning of the SOP, which was timed to coincide with the start of the annual soil moisture depletion phase. By 16 June (Fig. 5), the agricultural fields had become significantly drier with brightness temperatures ranging from 270 K to 285 K. Surface soil moisture in the oat field (N2 in Fig. 3) is distinct from the adjacent maize field (N3) in this image. By 2 July (Fig. 6), the oat field was near harvest and appears to be one of the driest portions of the image. Brightness temperatures in Figure 6 show that the agricultural fields are still as dry as in Figure 5, except for small localized wet areas that reflect recent irrigation. The independently digitized field boundaries shown in each image appear to delineate the PBMR data spatially.

Emissivity Computation and Analysis

The remotely sensed parameter most closely related to surface soil moisture is emissivity. Computation of emissivity requires measurements of both brightness temperature (microwave) measured by the PBMR and surface temperature (thermal infrared). Surface temperature has generally been estimated in previous use of the PBMR by PRT-5 radiometer measurements. This

sensor provides an excellent measurement of surface temperature for a small beam centered at the nadir, serving as an acceptable estimate for approximately homogeneous land surfaces. However, land surfaces in the HAPEX-MOBILHY grid were disjointed, heterogeneous arrangements of agricultural fields and forest. In such an environment, use of the PRT-5 in conjunction with the PBMR was not straight forward. It was not difficult to conceive of situations where the PRT-5 measured completely different fields than those measured by an outside PBMR beam. Such events would lead to erroneous estimates of emissivity. The error is a function of the difference between the PRT-5 temperature and the actual surface temperature for the area viewed by an outside PBMR beam (i.e., beams 1 or 4).

Emissivity was therefore not computed with simultaneous PBMR and PRT-5 measurements at every position along the flight line. Instead, "field-averaged" values of each sensor's respective observations were computed for the calibration fields (N0, N1, . . . , N5). Passive microwave data recorded by the PBMR were extracted from brightness temperature images for the six fields. PRT-5 data were treated as line transects, and all data from those portions of the transect that were recorded over a given calibration field were averaged to estimate the mean surface temperature of that field.

An example of a line transect from Lubbon is shown in Figure 7. Notice that the field boundaries match the temperature transitions of the transect. To obtain the mean brightness temperature for a calibration field, the pixel values for that field were extracted from the PBMR imagery and averaged. The ratio of the mean brightness temperature to the mean surface temperature for a given calibration field on a given date constituted the "field-averaged emissivity." This computed quantity was

examined using linear regression techniques to explore the relationship between emissivity and surface soil moisture for these data.

The field-averaging approach circumvented problems caused by the PRT-5 sensor's limited view area. However, it did not substitute for a completely image-based approach because it was not possible to develop emissivity images. In an image-based approach, a thermal image of the same spatial scale as the brightness temperature images would be required. Emissivity would be computed by pixel, dividing the brightness temperature pixel values by corresponding thermal pixel values. The result would be a map of emissivity, showing the spatial variation of individual fields rather than just a mean value. Lack of thermal imagery prevented generation of soil moisture maps based on emissivity. A more spatially distributed measurement of surface temperature would have been required for this purpose, such as that provided by the TIMS. TIMS data were collected in the HAPEX-MOBILHY experiment, but were not available during the course of this study.

The regression between field-averaged emissivity and field-averaged surface soil moisture is depicted in Figure 8 as a dashed line. The coefficient of determination for this regression was 0.32, indicating a weak linear relationship. Of the six fields represented in Figure 8, only the oat field (N2) had a vegetation canopy mature enough to attenuate the microwave signal appreciably during the SOP. The significance of the oat biomass compared to the other fields is shown by the biomass sample measurements in Table 3. The regression line for data from all calibration fields except N2 is depicted in Figure 8 as a solid line. Removal of possible vegetation attenuation effects did not improve the strength of the regression ($r^2 = 0.25$).

Figure 7. East-west line transect of surface temperatures at Central Site Lubbon measured by the PRT-5 sensor on a 300 m (above-ground level) flight on 31 May 1986. Field boundaries normal to the flight line are delineated in the figure.

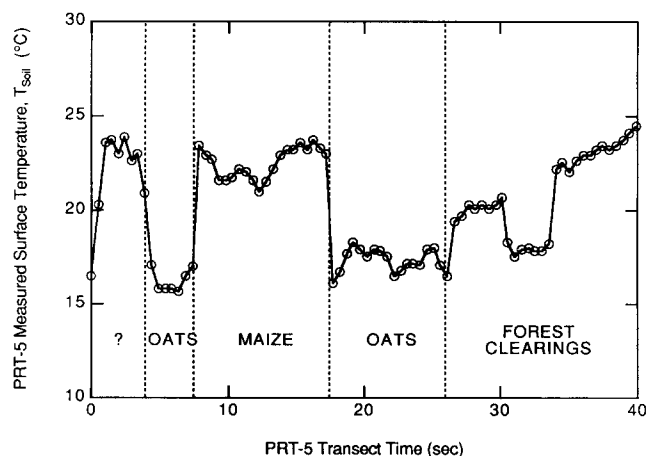


Figure 8. Regression between field-averaged emissivity calculations (based on remote sensing measurements) and field-averaged gravimetric surface soil moisture measurements collected during the HAPEX-MOBILHY SOP.

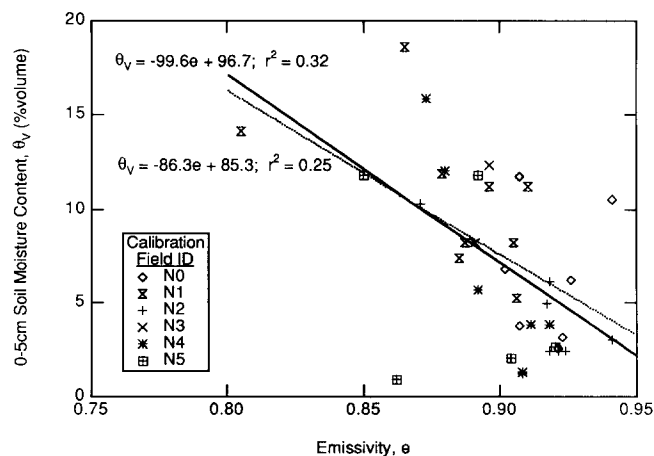


Table 3. Calibration Field Vegetation and Biomass Samples

| Date | Field | Vegetation | Dry Biomass (g / m ²) | Wet Biomass (g / m ²) |
|---------|-------|-----------------|--------------------------------------|--------------------------------------|
| 13 June | N0 | Maize | 17 | 139 |
| | N1 | Forest clearing | — | — |
| | N2 | Oats | 1728 | 8336 |
| | N3 | Maize | — | — |
| | N4 | Maize | 56 | 450 |
| | N5 | Maize | 41 | 350 |
| 22 June | N0 | Maize | 259 | 1034 |
| | N1 | Forest clearing | 16 | 50 |
| | N2 | Oats | — | — |
| | N3 | Maize | 1650 | 6894 |
| | N4 | Maize | 180 | 890 |
| | N5 | Maize | 150 | 1057 |
| 26 June | N0 | Maize | 103 | 1014 |
| | N1 | Forest clearing | — | — |
| | N2 | Oats | 1510 | 5274 |
| | N3 | Maize | — | — |
| | N4 | Maize | 114 | 820 |
| | N5 | Maize | 164 | 1500 |

Brightness Temperature and Surface Soil Moisture

Because it was not possible to develop emissivity imagery with available data, the regression analysis was repeated for brightness temperature and surface soil moisture data. This regression, if adequate, would provide an equation for use in converting brightness temperature images into soil moisture maps. Brightness temperature alone has been compared to surface soil moisture in previous research with the PBMR (Schmugge et al., 1988; Jackson and Schmugge, 1986). The relationship and data reported by Schmugge et al. (1988) for the Konza Prairie are depicted in Figure 9. Unburned watershed data reported by Schmugge et al. (1988) were not included because of the microwave attenuation properties of the unburned grasslands where a thatch layer had developed.

The analysis procedure followed by Schmugge et al. (1988) was repeated for the HAPEX-MOBILHY data. Brightness temperature data were extracted for the six calibration fields from the brightness temperature images. Using summary statistics for these fields (Table 4a and 4b) and frequency histograms, each calibration field was individually inspected before inclusion in the regression analyses. The regression between the average volumetric soil moisture (from Tables 1 and 2) and the average calibration field brightness temperature are depicted in Figure 9. Each of the six calibration fields was assigned a unique symbol in Figure 9 to aid in analysis. Notice that the range of soil moisture observed in the HAPEX-MOBILHY data collection ranged from around 20% (volumetric basis) to nearly zero. This dry condition was in sharp contrast to the Konza data shown

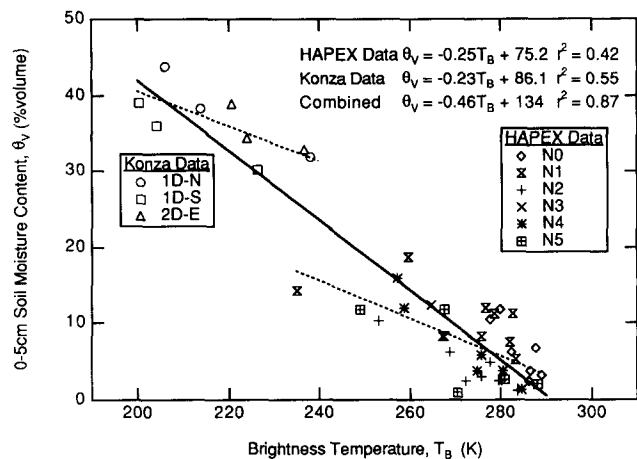


Figure 9. Plot of field-averaged PBMR brightness temperature measurements versus field-averaged gravimetric surface soil moisture measurements collected in 1986 at the Konza Prairie Reserve (burned watersheds only) and in the HAPEX-MOBILHY SOP. Regression lines for each data set alone and for the combined data set are indicated.

in Figure 9, which ranged from 20% to 50% (volumetric basis).

In neither data collection was an exceptional fit indicated by the coefficient of determination (r^2). The limited range of observed emissivity values, or, alternatively, the limited range of surface soil moisture, suggests that the poor linear fit may be a result of examining too narrow a range for which the expected relationship is defined. When the range of a predictor variable (x) is narrow, the variation in the predicted variable (y), ignoring x , is not much greater than the variation in y given x . In these cases summary statistics such as r^2 can be misleading (Weisberg, 1985), that is, a low r^2 would not necessarily mean that a linear relationship is inappropriate.

The least-squares linear regression equations obtained describing surface soil moisture as functions of brightness temperature and emissivity for the HAPEX-MOBILHY data were

$$\theta_v = -0.25T_b + 75.2 \quad (2)$$

and

$$\theta_v = -86.3e + 85.3, \quad (3)$$

where θ_v is the soil moisture (volumetric basis) as a percent, T_b is the brightness temperature (K), and e is the emissivity (dimensionless).

To gain perspective on the result of the narrow range of observed soil moisture, the Konza Prairie and HAPEX-MOBILHY PBMR brightness temperature data were combined and examined. Because the Konza Prairie conditions during the FIFE experiment tended to be wet, while the HAPEX-MOBILHY SOP conditions

Table 4a. Summary Statistics for PBMR Brightness Temperature Pixels
Extracted from Central Site Lubbon Images, Calibration Fields
N0–N5 for Day of Year (DOY) 149–167^a

| DOY | Statistic | N0 | N1 | N2 | N3 | N4 | N5 |
|--------|-----------|--------|--------|--------|--------|--------|--------|
| 86D149 | <i>n</i> | 173 | 1245 | 1917 | 4091 | 1429 | 782 |
| | \bar{x} | 253.38 | 252.42 | 254.39 | 250.97 | 248.34 | 252.30 |
| | <i>s</i> | 0.904 | 7.391 | 5.846 | 4.650 | 5.897 | 4.148 |
| 86D151 | <i>n</i> | 1337 | 958 | 2061 | 3458 | 910 | 388 |
| | \bar{x} | 275.52 | 257.32 | 260.99 | 264.84 | 252.43 | 266.28 |
| | <i>s</i> | 3.211 | 7.054 | 3.146 | 3.774 | 6.296 | 1.891 |
| 86D154 | <i>n</i> | 396 | 846 | 1988 | 3738 | 1319 | 672 |
| | \bar{x} | 272.10 | 259.56 | 263.65 | 267.23 | 257.16 | 267.75 |
| | <i>s</i> | 2.333 | 6.832 | 4.751 | 3.605 | 6.180 | 3.153 |
| 86D157 | <i>n</i> | 1529 | 1175 | 1884 | 3974 | 1088 | 536 |
| | \bar{x} | 258.91 | 235.10 | 253.04 | 249.10 | 242.38 | 248.95 |
| | <i>s</i> | 2.941 | 7.532 | 3.025 | 3.409 | 8.704 | 4.741 |
| 86D165 | <i>n</i> | 906 | 1211 | 2639 | 4674 | 1365 | 410 |
| | \bar{x} | 279.75 | 267.59 | 268.80 | 278.03 | 274.68 | 278.92 |
| | <i>s</i> | 4.225 | 5.735 | 3.843 | 2.593 | 2.793 | 1.126 |
| 86D167 | <i>n</i> | 1323 | 1255 | 1793 | 3336 | 801 | 474 |
| | \bar{x} | 287.75 | 276.70 | 277.66 | 285.68 | 283.25 | 287.93 |
| | <i>s</i> | 3.418 | 5.659 | 3.030 | 3.233 | 3.048 | 1.962 |

^a *n* = number of samples (pixels), \bar{x} = mean, and *s* = standard deviation.

Table 4b. Summary Statistics for PBMR Brightness Temperature Pixels
Extracted from Central Site Lubbon Images, Calibration Fields
N0–N5 for Day of Year (DOY) 169–183^a

| DOY | Statistic | N0 | N1 | N2 | N3 | N4 | N5 |
|--------|-----------|--------|--------|--------|--------|--------|--------|
| 86D169 | <i>n</i> | 1496 | 1249 | 1988 | 3282 | 1194 | 630 |
| | \bar{x} | 282.31 | 275.94 | 272.26 | 283.31 | 280.39 | 280.86 |
| | <i>s</i> | 6.963 | 6.841 | 6.444 | 2.658 | 2.939 | 3.697 |
| 86D174 | <i>n</i> | 1544 | 1257 | 1711 | 3425 | 898 | 426 |
| | \bar{x} | 283.81 | 278.52 | 274.43 | 279.21 | 281.10 | 277.76 |
| | <i>s</i> | 4.698 | 4.175 | 3.849 | 9.191 | 3.28 | 6.436 |
| 86D176 | <i>n</i> | 1495 | 906 | 1924 | 3022 | 1004 | 423 |
| | \bar{x} | 289.09 | 283.22 | 280.20 | 283.86 | 284.56 | 270.46 |
| | <i>s</i> | 3.578 | 4.904 | 9.913 | 6.807 | 3.031 | 13.992 |
| 86D178 | <i>n</i> | 1523 | 1216 | 2007 | 3545 | 1183 | 557 |
| | \bar{x} | 286.12 | 282.60 | 279.50 | 279.02 | 275.75 | 275.76 |
| | <i>s</i> | 6.133 | 4.415 | 9.036 | 10.735 | 8.174 | 5.158 |
| 86D181 | <i>n</i> | 1461 | 564 | 2298 | 3663 | 1329 | 335 |
| | \bar{x} | 277.49 | 260.12 | 275.65 | 266.93 | 258.86 | 263.42 |
| | <i>s</i> | 4.441 | 4.449 | 4.852 | 8.574 | 7.553 | 3.763 |
| 86D183 | <i>n</i> | 748 | 1039 | 2297 | 4537 | 1166 | 375 |
| | \bar{x} | 286.51 | 282.07 | 283.67 | 276.04 | 275.80 | 279.50 |
| | <i>s</i> | 4.620 | 4.006 | 4.793 | 9.435 | 7.524 | 5.215 |

^a *n* = number of samples (pixels), \bar{x} = mean, and *s* = standard deviation.

were very dry, the range of the combined data set was large. The combined data set is shown in Figure 9. Although it would be satisfying to apply the regression resulting in $r^2 = 0.89$, physical reservations with respect to the differences in soil types argued against this. This exercise illustrates that a large range of measured soil

moisture values may be required to adequately define the linear relationship between passive microwave measurements and surface soil moisture. Noise in both remote- and ground-based measurement systems will tend to mask the underlying linear relationship for narrow ranges of soil moisture.

Soil Moisture Mapping

It was not possible to produce accurate surface soil moisture maps from the PBMR data for two reasons. First, spatial limitations of PRT-5 temperature data prevented computation of spatially distributed emissivity values. Second, local calibration efforts produced poor descriptions of the relationship between surface soil moisture and emissivity or brightness temperature. However, it is worthwhile to demonstrate the potential of PBMR data and techniques for its use. Approximate surface soil moisture images were produced by applying approximate relations between brightness temperature and surface soil moisture to brightness temperature data. Curves calculated using standard Fresnel equation (Dobson et al., 1985) relating surface soil moisture to emissivity were rewritten in terms of brightness temperature to provide the approximate relations. While little confidence can be placed in the absolute values of soil moisture in these images, the values should be correct on a relative scale.

Figures 10, 11, and 12 show three images of soil moisture, with values ranging from zero to 30% at Central Site Lubbon for 29 May, 16 June, and 2 July 1986, respectively. The gray scale is the reverse of that used in brightness temperature imagery so that dark still indicates wet conditions and light represents dry conditions.

Brightness temperature data were classified according to canopy cover so that different vegetation factors could be treated appropriately. For Central Site Lubbon, data were classified as either forest, oats, or agricultural (nonoats). Forested areas were excluded from the soil moisture images because the forest canopy totally attenuated the microwave signal from the soil. Oats were segregated from other agricultural crops because of their maturity in this period. Except for oats, agricultural crops were young enough to treat as bare soil for our analysis.

Figure 10. Surface soil moisture map of Central Site Lubbon on 29 May 1986.

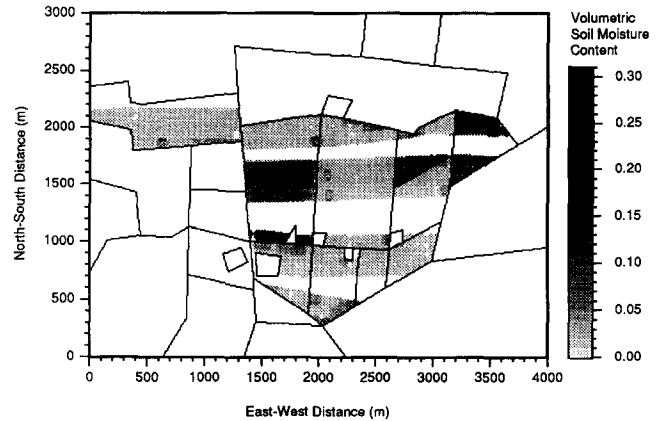
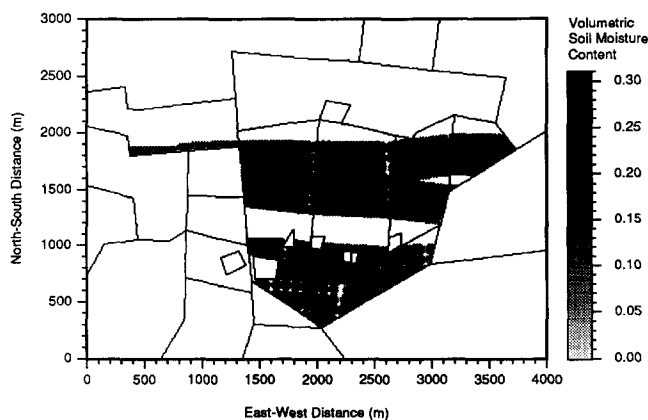


Figure 11. Surface soil moisture map of Central Site Lubbon on 16 June 1986.

Emissivity values were not available because of the problems encountered in extending PRT-5 data to the spatial scale of PBMR data. A set of emissivity values was generated over a range of soil moisture values using the Fresnel equations (Dobson et al., 1985) with a roughness factor of 0.1 [chosen because it introduces a small level of roughness found appropriate in working with the Konza data (Wang et al., 1990)]. The regression fit for over these values for bare soil is

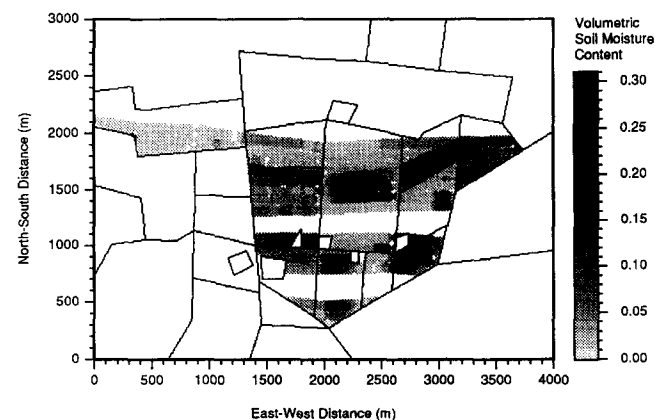
$$e = 0.941 - 0.816\theta_v \quad (4a)$$

Similarly, the regression equation for the same soil and roughness and vegetation biomass representative of the oat canopy is

$$e = 0.967 - 0.459\theta_v \quad (4b)$$

Recall that emissivity for bare soils is equal to the ratio of T_b and T_{soil} . To generate a relationship between brightness temperature and surface soil moisture, an effective surface temperature was assumed ($T_{soil} = 300$ K). Substituting the assumed value for T_{soil} ,

Figure 12. Surface soil moisture map of Central Site Lubbon on 2 July 1986.



$$e = \frac{T_b}{T_{soil}} = \frac{T_b}{300} \quad (5)$$

Substituting Eq. (5) into Eq. (4),

$$\frac{T_b}{300} = 0.941 - 0.816\theta_v, \quad (6a)$$

$$\frac{T_b}{300} = 0.967 - 0.459\theta_v. \quad (6b)$$

Rearranging Eq. (6) to express in terms of soil moisture, we obtain

$$\theta_v = 1.1532 - 0.0041T_b, \quad (7a)$$

$$\theta_v = 2.1068 - 0.0073T_b. \quad (7b)$$

Using Eq. (7), all pixel values of T_b in the brightness temperature images were converted to effective emissivity. The resulting approximate soil moisture images are shown in Figures 10, 11, and 12, corresponding to the brightness temperature data shown in Figures 4, 5, and 6.

The soil moisture values indicated in Figures 10, 11, and 12 tend to be very dry, usually less than 10% (volumetric basis). Figure 10, corresponding to 29 May, displays wetter conditions and more variation than the two latter dates, and the distinctly wetter conditions of the oat field (field N2 in Fig. 3). Another oat field in the upper right corner of the mapped area displays similar conditions. The remaining fields were planted in maize and exhibit drier conditions in Figure 10. By 16 June (Fig. 11), the oat fields are still slightly wetter than the surrounding fields, but all mapped areas have dried considerably. Fairly uniform, dry conditions prevail in all agricultural fields mapped on 2 July (Fig. 12) except for the irrigated areas in field N3.

CONCLUSIONS AND RECOMMENDATIONS

Passive microwave mapping of surface soil moisture produced mixed results. The PBMR detected spatial and temporal variation of surface microwave emissions during the HAPEX-MOBILHY SOP with a surprising degree of definition and clarity. However, attempts to relate these data to ground measurements of surface soil moisture gave poor results. The strength of the linear regression fit was expressed by the coefficient of determination (r^2). The coefficient of determination for the regression between surface soil moisture and emissivity was 0.32, while for the regression between surface soil moisture and brightness temperature it was 0.43.

Aside from noise (experimental error) in the measurements, two factors contributed in large part to the scatter observed in the microwave versus soil moisture relationship: 1) an inadequate range of observed surface soil moisture conditions in the calibration fields during the experiment and 2) a limited ground-truth data set.

The narrow range of surface soil moisture values observed in the HAPEX-MOBILHY SOP was made apparent by comparison with FIFE data. As for ground-truth data, only four samples were collected from each calibration field (see Table 1) in the vicinity of Central Site Lubbon on each overflight date. These four samples were used to represent the mean surface soil moisture of the fields sampled. Unfortunately, the high degree of variation in these sample values suggests that four was an insufficient number for this purpose, possibly due to the inherent spatial variation of soil moisture within individual fields. Recommendations for addressing these factors in future research efforts are in order. For a limited, dry range of surface soil moisture, two options are available. If the limited range is expected in an experiment conducted during the annual soil moisture depletion period for an area, one mission could be flown earlier together with appropriate ground data collection to obtain a "wet" data set. Although this solution may seem reasonable, it may involve prohibitive costs in aircraft operation or problems with aircraft availability and priority. A second option involves the use of an irrigated field in the experiment. Such a field could be irrigated to field capacity 1 day before a flight mission to provide the wet data set. This option would not interfere with aircraft operations, though close coordination with irrigators must be ensured. For a limited range of soil moisture in the wet end of the curve, the only option is to fly a mission at a different time when dry conditions are prevalent, though this is not crucial because we know what to expect at the dry end of the curve.

The second factor, an inadequate ground-truth data set, can be handled through improved sampling techniques. Ground data collection efforts will always involve limitations in time, human resources, and budget. While the PMBR imagery and even PRT-5 transect allow for quantification of the distribution of observed variables over each calibration field, the limited ground-truth data collected precludes quantification of a corresponding distribution for gravimetric surface soil moisture. Developments of new instrumentation to replace or augment laborious gravimetric techniques, including time domain reflectometry and capacitance probes, are seen as possible solutions to the problem of limited surface soil moisture samples (Roth et al., 1990; Heimo-vaara and Bouten, 1990). These two techniques are being scheduled for testing and application in the HAPEX-SAHEL experiment to be performed in the arid sub-Saharan region of Niger in 1992.

The use of a spatially distributed remote measurement of surface kinetic temperature is recommended for all future work over heterogeneous, disjointed land surfaces with the PBMR. The small view area of the PRT-5 was spatially inadequate for estimating surface temperature in the area of interest, limiting our ability

to compute emissivity with PBMR data. TIMS sensor data are available and would meet this requirement if additional research efforts are made with HAPEX-MOBILHY PMBR data.

The authors thank Larry Mahrt and Wayne Gibson of the Department of Atmospheric Sciences, Oregon State University, for extending assistance and VAX computer time for PBMR data transfer. This study was funded under USDA-ARS Specific Cooperative Agreement Number 58-3K47-9-006, "Water Budget Studies with HAPEX-MOBILHY." Work was conducted both at the USDA-ARS Hydrology Laboratory and at Oregon State University. Additional publication support was provided by Pacific Northwest Laboratories, operated for the U.S. Department of Energy by Battelle Memorial Institute under Contract DE-AC06-76RLO 1830.

REFERENCES

- André, J. C., Goutorbe, J. P., and Perrier, A. (1986), HAPEX-MOBILHY: a hydrological atmospheric experiment for the study of water budget and evaporation at the climatic scale, *Bull. Meteorol. Soc.* 67:134-144.
- André, J. C., Goutorbe, J. P., Perrier, A., et al. (1988), Evaporation over land surfaces. First results from HAPEX-MOBILHY Special Observing Period, *Ann. Geophys.* 6: 477-492.
- Bessemoulin, P. G., Desroziers, G., Payen, M., and Tarrieu, C. (1987), *Atlas des données SAMER*, Centre National de Recherches Météorologiques Report, Toulouse, France, 256 pp.
- Dobson, M. C., Ulaby, F. T., Halli Kainen, M. T., and Reyes, M. (1985), Microwave dielectric behavior of wet soil: Part II. dielectric mixing models, *IEEE Trans. Geosci. Remote Sens.* GE-23:35-46.
- Jackson, T. J., and O'Neill, P. E. (1987), Salinity effects on the microwave emissions of soils, *IEEE Trans. Geosci. Remote Sens.* GE-25(2):214-220.
- Jackson, T. J., Hawley, M. E., Shuie, J., et al. (1986), Assessment of pre-planting soil moisture using airborne microwave sensors, in *Hydrologic Applications of Space Technology*, IAHS Publication 160, pp. 111-118.
- Jackson, T. J., and Schmugge, T. J. (1986), Passive microwave remote sensing of soil moisture, in *Advances in Hydroscience*, Academic, Washington, DC, Vol. 14, pp. 123-159.
- Heimovaara, T. J., and Bouten, W. (1990), A computer-controlled 36-channel time domain reflectometry system for monitoring soil water contents. *Water Resour. Res.* 26(10):2311-2316.
- Goutorbe, J.-P., Noilhan, J., Valancogne, C., and Cuenca, R. H. (1989), Soil moisture variations during HAPEX-MOBILHY, *Ann. Geophys.* 7(4):415-426.
- Nichols, W. E. (1989), Land surface energy balance and surface soil moisture variation in HAPEX-MOBILHY, M.S. thesis, Oregon State Univ., Corvallis.
- Roth, K., Schulm, R., Flüher, H., and Attinger, W. (1990), Calibration of time domain reflectometry for water content measurement using a composite dielectric approach, *Water Resour. Res.* 26(10):2267-2273.
- Schmugge, T. J., Wang, J. R., and Asrar, G. (1988), Results from the push broom microwave radiometer flights over the Konza Prairie in 1985, *IEEE Trans. Geosci. Remote Sens.* 26(5):590-596.
- Theis, S. W., and Blanchard, A. J. (1988), The effects of measurement error and confusion from vegetation on passive microwave estimates of soil moisture, *Int. J. Remote Sens.* 9(2):333-340.
- Wang, J. R., Shiue, J. C., Schmugge, T. J., and Engman, E. T. (1989), Mapping surface soil moisture with L-band radiometric measurements, *Remote Sens. Environ.* 27:305-312.
- Wang, J. R., Shiue, J. C., Schmugge, T. J., and Engman, E. T. (1990), The L-band PBMR measurements of surface soil moisture in FIFE, *IEEE Trans. Geosci. Remote Sens.* 28(5): 906-914.
- Weisberg, S. (1985), *Applied Linear Regression*, Wiley, New York, 324 pp.